

Intelligent identification of two-dimensional nanostructures by machine-learning optical microscopy

Xiaoyang Lin^{1,2,§} (✉), Zhizhong Si^{1,§}, Wenzhi Fu^{3,§}, Jianlei Yang^{3,§}, Side Guo¹, Yuan Cao¹, Jin Zhang⁴, Xinhe Wang^{1,4}, Peng Liu⁴, Kaili Jiang⁴, and Weisheng Zhao^{1,2} (✉)

¹ Fert Beijing Research Institute, School of Microelectronics & Beijing Advanced Innovation Center for Big Data and Brain Computing (BDBC), Beihang University, Beijing 100191, China

² Beihang-Goertek Joint Microelectronics Institute, Qingdao Research Institute, Beihang University, Qingdao 266000, China

³ Fert Beijing Research Institute, School of Computer Science and Engineering & Beijing Advanced Innovation Center for Big Data and Brain Computing (BDBC), Beihang University, Beijing 100191, China

⁴ State Key Laboratory of Low-Dimensional Quantum Physics, Department of Physics & Tsinghua-Foxconn Nanotechnology Research Center, Collaborative Innovation Center of Quantum Matter, Tsinghua University, Beijing 100084, China

[§] Xiaoyang Lin, Zhizhong Si, Wenzhi Fu, and Jianlei Yang contributed equally to this work.

Received: 14 April 2018

Revised: 20 July 2018

Accepted: 23 July 2018

© Tsinghua University Press and Springer-Verlag GmbH Germany, part of Springer Nature 2018

KEYWORDS

machine-learning
optical identification,
two-dimensional (2D)
material,
heterostructure,
artificial intelligence

ABSTRACT

Two-dimensional (2D) materials and their heterostructures, with wafer-scale synthesis methods and fascinating properties, have attracted significant interest and triggered revolutions in corresponding device applications. However, facile methods to realize accurate, intelligent, and large-area characterizations of these 2D nanostructures are still highly desired. Herein, we report the successful application of machine-learning strategy in the optical identification of 2D nanostructures. The machine-learning optical identification (MOI) method endows optical microscopy with intelligent insight into the characteristic color information of 2D nanostructures in the optical photograph. The experimental results indicate that the MOI method enables accurate, intelligent, and large-area characterizations of graphene, molybdenum disulfide, and their heterostructures, including identifications of the thickness, existence of impurities, and even stacking order. With the convergence of artificial intelligence and nanoscience, this intelligent identification method can certainly promote fundamental research and wafer-scale device applications of 2D nanostructures.

1 Introduction

Two-dimensional (2D) materials have attracted increasing interest owing to their superior properties

[1–3]. Heterostructures of 2D materials, which enable great flexibility in both junction fabrication and property engineering, have further triggered revolutions in corresponding device applications [4–7]. Considering

Address correspondence to Xiaoyang Lin, XYLin@buaa.edu.cn; Weisheng Zhao, weisheng.zhao@buaa.edu.cn

the progress in wafer-scale synthesis method [8–10], the development of an efficient and large-area characterization technique has been a primary obstacle for fundamental research and commercial level applications of 2D nanostructures. Among the existing techniques, transmission electron microscopy and scanning tunneling microscopy (STM) enables characterization with high spatial resolution down to the atomic scale [11–14]. However, both these techniques have drawbacks of low-throughput and complicated sample preparation. Atomic force microscopy (AFM) with special design can also enable atomic characterization of 2D materials and even the interface of 2D heterostructures; however, the efficiency of this technique is limited by the presence of surface adsorbates [15, 16]. Optical spectroscopy, for example, Raman spectroscopy, can realize accurate characterization of 2D nanostructures [17]. However, the spectroscopy method usually enables local characterization within the light spot, resulting in limited efficiency. Compared to the aforementioned techniques, optical microscopy methods, which enable high-speed, large-area, non-destructive, and accurate identification of samples from as-collected optical photographs (i.e., the ability of wide-field characterization), have already boosted controllable synthesis or fabrication, structure-dependent physical property measurement, and device applications of 2D nanostructures [18–24].

The optical microscopy method by characterizing bright-field photographs of 2D materials has been applied for large-area or even wafer-scale characterization of 2D materials [7–8, 23–26]. Recently, identification of interlayer coupling in 2D vertical heterojunctions has successfully extended this characterization method to 2D heterostructures, although it relies on a modified optical microscope with ability of photoluminescence imaging [27, 28]. However, there are still two drawbacks: (1) Identification of 2D heterostructures by optical microscopy is still immature; (2) the optical microscopy method often relies on the experience of the user. Unless intelligent image processing and identification of 2D nanostructures are realized, these drawbacks can greatly hamper its applications. Adoption of machine-learning strategy in image identification or visual

recognition has achieved distinct advantages and outperformed humans, implying the great potential of artificial intelligence in image identification of micro and especially nanostructures [29, 30]. In this sense, integration of machine-learning with optical microscopy may realize accurate, intelligent, and large-area characterization of 2D materials and even 2D heterostructures, which can further promote both fundamental research and commercial applications.

In this work, we applied machine-learning strategy in the optical identification of 2D nanostructures, including graphene, molybdenum disulfide (MoS_2), and heterostructures of these two materials. The machine-learning optical identification (MOI) method relies on trainable and automatic analyses of red, green, and blue (RGB) information in the optical photograph of 2D nanostructures using a support vector machine (SVM) algorithm. With this intelligent insight into the characteristic color information of 2D nanostructures, the MOI method enables accurate and intelligent characterization of 2D nanostructures, including identification of thickness, existence of impurities, and even stacking order, which is expected to promote the development of 2D science and technology.

2 Experimental

The MOI system is based on an optical microscope system enhanced by self-customized software (Fig. 1). The optical microscope enables collection of bright-field photographs of 2D nanostructures at different magnifications. The self-customized software further realizes intelligent identification of the as-collected photographs according to a pre-established database and model. The intelligent identification can be sorted in two steps (Fig. 1), i.e., a training process and a test process. The purpose of the training process is to establish a database and the corresponding SVM model containing the “fingerprint” or characteristic information of RGB channel intensities in the optical photograph of 2D materials with different thicknesses. During the training process, the RGB data in the optical microscope photographs of graphene or MoS_2 samples at different light intensities (“training set” in Fig. 1), is manually linked to graphene or MoS_2 with

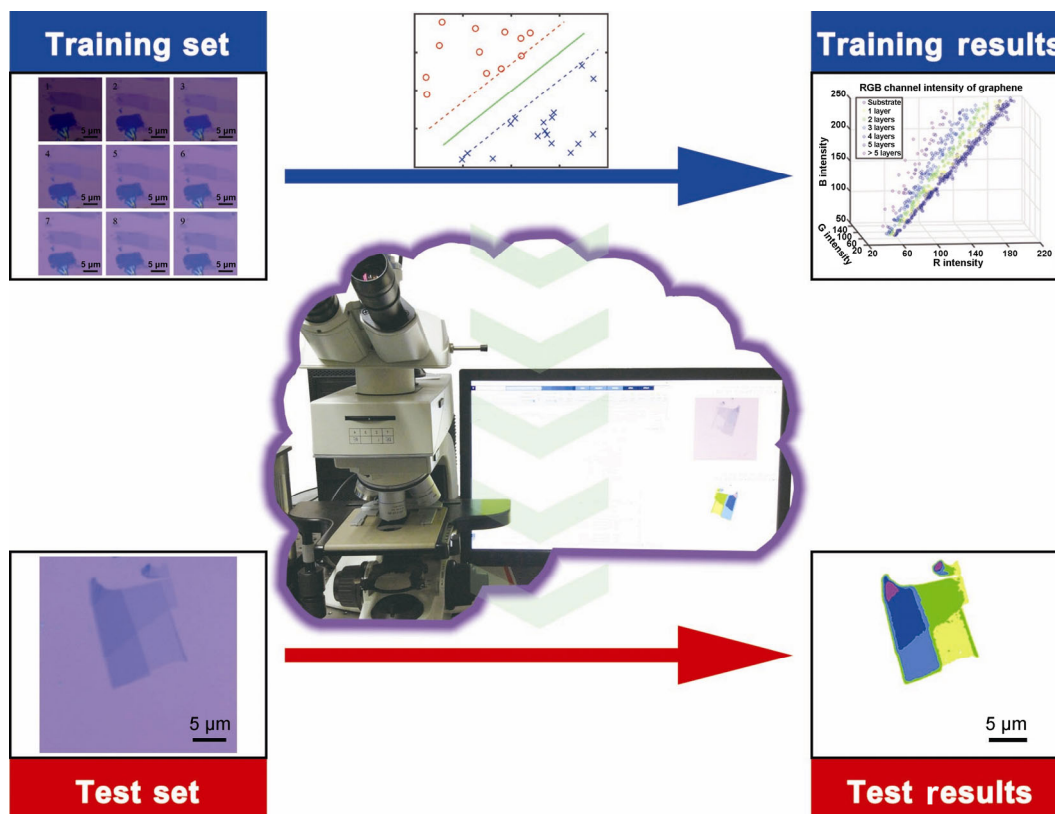


Figure 1 The MOI system. Schematic illustration and photograph of the MOI system. The training set contains optical microscope photographs of graphene or MoS₂ samples at different light intensities. Following the judgment of AFM and Raman spectroscopy, the RGB database and SVM model of graphene or MoS₂ samples (denoted as “training results”) are established after SVM analyses of the RGB data collected from the training set. Referring to the “training results”, graphene, MoS₂, or heterostructures of these two materials can be identified according to their optical microscope photograph (denoted as “test results”). The brain shaped inset shows the photograph of the MOI system which includes an optical microscope enhanced by self-customized software.

different number of layers and then classified into different categories by an SVM algorithm, following the judgments of AFM and Raman spectroscopy. The database and the SVM model with different categories of RGB channel intensities linked to the sample thickness (“training result” in Fig. 1) thus make the following test process possible. During the test process, the RGB information in the photographs of graphene or MoS₂ (“test set” in Fig. 1) is collected and classified by the software into specific categories. These classifications result in a false-color image (“test result” in Fig. 1), which indicates the distribution of substrate, 2D material (with different numbers of layers), and even impurities. Such a self-customized system inheriting the *in situ* and the wide-field characterization features of optical microscopy thus enables accurate, intelligent, and large-area identification of 2D nanostructures.

The accurate and intelligent identification relies on the optical contrast characteristics of the 2D materials [19–22] as well as the efficient processing and recognition by the self-customized software [29, 30]. The following key features of the MOI system greatly improve the performance of identification. The first one is the pretreatment of the photographs before analysis. The pretreatment includes denoising by mean filtering and median filtering, together with color calibration by linear scaling of G and B channels according to the R channel of the substrate. The color calibration eliminates possible influence induced by the instability of the optical microscope system. The second feature is about the SVM algorithm. For a small set of training samples, the SVM algorithm is an efficient supervised learning model for data classification [31]. In the MOI system, the SVM classifiers represent the training data of RGB information in

a three-dimensional (3D) space (see Fig. S1 in the Electronic Supplementary Material (ESM)), and decide the maximum-margin planes (i.e., boundaries of different categories). After mapping the testing sample into the same space, the maximum-margin plane is evaluated to perform the classification into a specific category (e.g., single-layered graphene). The third feature is to perform the identification by multi-channel information of RGB data rather than judging the number of layers by only one channel. Unlike conventional identification methods based on the contrast difference of specific channel between the substrate and the 2D material [22, 32], which have the disadvantage of spatial inhomogeneity of the light intensity, our multi-channel identification method realizes intelligent identification of 2D materials and their number of layers, as well as the substrate. Such a multi-channel identification method relies on the optical characteristics of 2D materials in RGB space (see Fig. S2 in the ESM for the results of graphene and MoS₂), which implies the possibility to simultaneously identify impurities, 2D materials, and even

2D heterostructures without the information of light intensity distribution in the optical microscope photograph.

3 Results and discussion

3.1 Identification of graphene

Accurate and intelligent identification of the graphene sample based on the MOI system is demonstrated in Fig. 2, which is expected to benefit abundant research and applications of graphene [2, 3]. In the training process, the optical microscope photographs of the graphene samples (see Figs. 2(a) and 2(c) for two typical samples) with deterministic judgment of the thickness by AFM (Figs. 2(b) and 2(d)) are processed as a database with different categories of RGB channel intensity linked to the sample thickness (i.e., different number of layers) and further analyzed by the SVM algorithm to establish a training model. The training result (i.e., the SVM model) contains as-classified RGB information of graphene and the

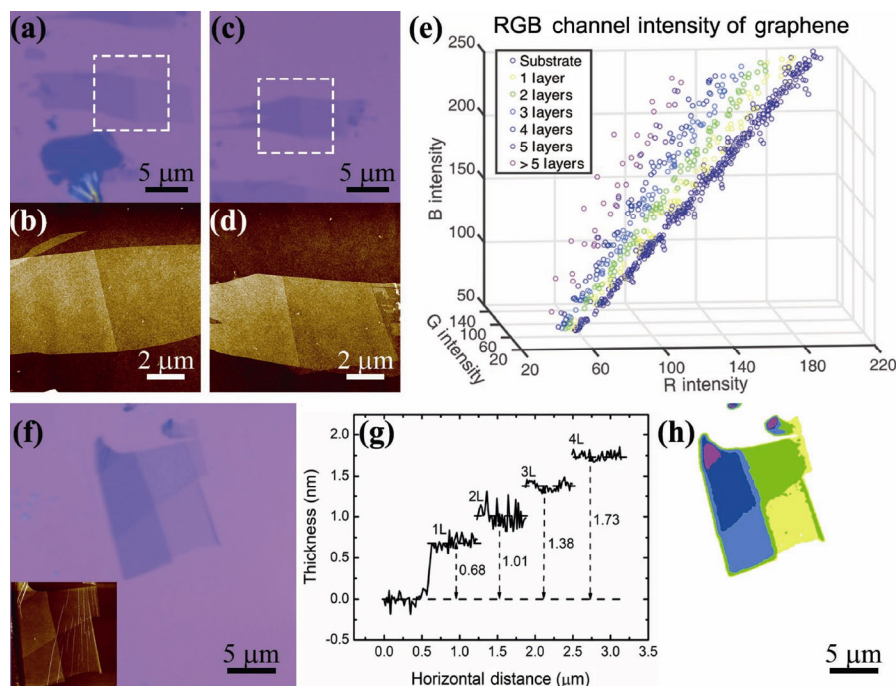


Figure 2 MOI of graphene sample. (a)–(d) Typical optical microscope photographs ((a) and (c)) included in the training set of graphene, including the corresponding AFM images ((b) and (d)). (e) Training result of graphene samples containing as-classified RGB information; note that the SVM model is not shown. (f) Optical microscope photograph of a mixed-layer graphene sample for test purpose; the inset shows the corresponding AFM image. (g) Thickness information of different-layer graphene in (f) by AFM analysis. (h) Test result of the sample in (f) according to the database in (e), where regions of different layers are colored in accordance with (e).

substrate (Fig. 2(e)), which enable the following intelligent identifications of graphene thickness. For a mixed-layer graphene sample (see Fig. 2(f) for the optical microscope photograph), the MOI system automatically refers the photograph to the training result by analyzing the RGB information. As shown in Fig. 2(h), accurate assignments of the number of graphene layers with a pixel-to-pixel accuracy of 96.78% are realized in agreement with the AFM results (insets of Figs. 2(f) and 2(g)), where regions of different layers are colored respectively.

3.2 Identification of MoS₂

In general, the MOI method also works for other 2D materials that have characteristics in RGB space, for example, MoS₂ and other transition metal dichalcogenides [19, 32]. Accurate and intelligent identification of MoS₂ sample is demonstrated in Fig. 3. Following a similar training process of graphene, the RGB information in the optical microscope photographs of MoS₂ samples (Figs. 3(a) and 3(c)) is collected and

analyzed by the SVM algorithm according to the thickness judgment by AFM measurements (Figs. 3(b) and 3(d)). As a result, a training result containing the characteristic RGB information of MoS₂ (Fig. 3(e)) is obtained. As shown in the false-color image in Fig. 3(h), intelligent identification of the MoS₂ sample is realized automatically with a pixel-to-pixel accuracy of 94.26% based on its optical microscope photograph (Fig. 3(f)). Besides, the intelligent identification result is also sensitive to impurities or contaminations (black regions in Fig. 3(h)) which can severely affect the intrinsic property of 2D materials [33, 34]. For example, adhesive residues appearing as light green regions on the substrate and encircling the MoS₂ flakes in the optical microscope photograph (Fig. 3(f)) can be successfully recognized.

3.3 Identification of 2D heterostructures

With great flexibility in junction fabrication and property engineering, heterostructures of 2D materials enable exploration of emerging 2D physics and novel

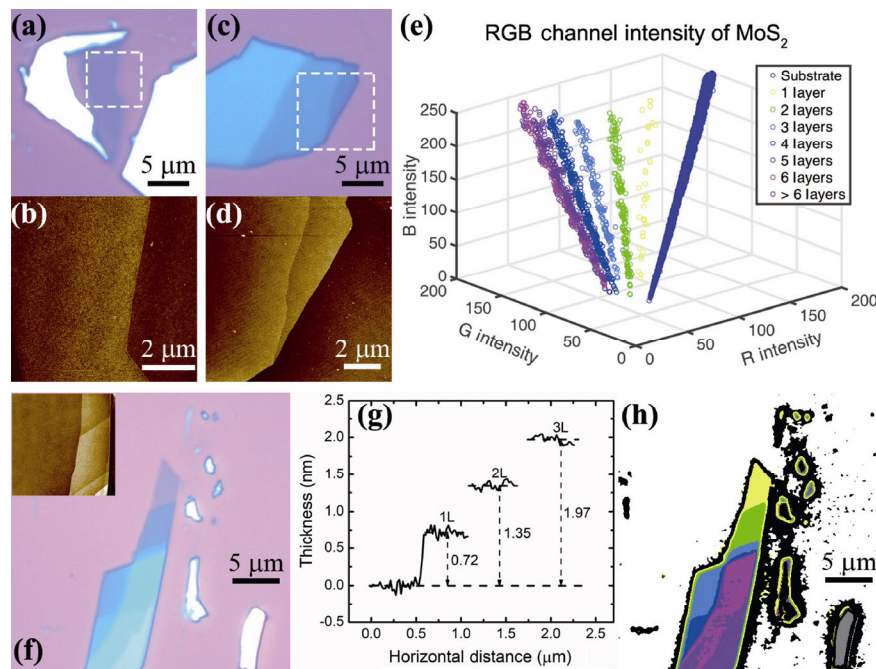


Figure 3 MOI of MoS₂ sample. (a)–(d) Typical optical microscope photographs ((a) and (c)) included in the training set of MoS₂, where corresponding AFM images ((b) and (d)) are also present. (e) Training result of MoS₂ samples containing as-classified RGB information; note that the SVM model is not shown. (f) Optical microscope photograph of a mixed-layer sample for test purpose; the inset shows the corresponding AFM image. (g) Thickness information of different-layer MoS₂ in (f) by AFM analysis. (h) Test result of the sample in (f) according to the database in (e), where regions of different layers are colored in accordance with (e). The as-identified regions of adhesive residues are blacked and the overexposed regions are grayed.

device applications [4–7]. Our intelligent identification method of 2D materials by their “fingerprints” in RGB channels may further realize the identification of 2D heterostructures and boost the development of 2D science. Figure 4(a) shows a 2D heterostructure with a vertical heterojunction of bilayer graphene and single-layered MoS₂, fabricated using a previously reported transfer method (see Ref. [35] for details of the transfer method). Based on the training results of graphene and MoS₂ samples (see Figs. 2(e) and 3(e), and Fig. S2 in the ESM), the intelligent identification of a graphene-MoS₂ heterostructure is successfully demonstrated (Fig. 4(c)).

Regions of substrate, graphene, MoS₂, heterojunction, as well as the resist residues from the transfer process can be automatically recognized with a pixel-to-pixel accuracy of 90.16%. Detailed analyses of the RGB information from different regions (Figs. 4(d) and 4(e)) indicate that MoS₂ dominates the optical contrast of the heterojunction, which can hamper accurate

identification of heterostructures by optical methods. According to the theoretical calculation results (see Fig. S3 in the ESM and Refs. [22, 36–38]), further optimization of the oxidation layer thickness and the light wavelength can be adopted to improve the performance of identification and even realize the identification of stacking order in the vertical heterojunction. Besides, further comparison of the RGB information before and after the transfer process (Fig. 4(e)) implies the feasibility of this intelligent identification method to evaluate the performance, especially the resist residues of the 2D material transfer method.

3.4 Discussion

Ever since the first application in the thickness identification of graphene [21, 22], much progress has been achieved in optical microscopy of 2D nanostructures [18–20, 27–29, 32, 39]. These breakthroughs include characterization capabilities of various 2D

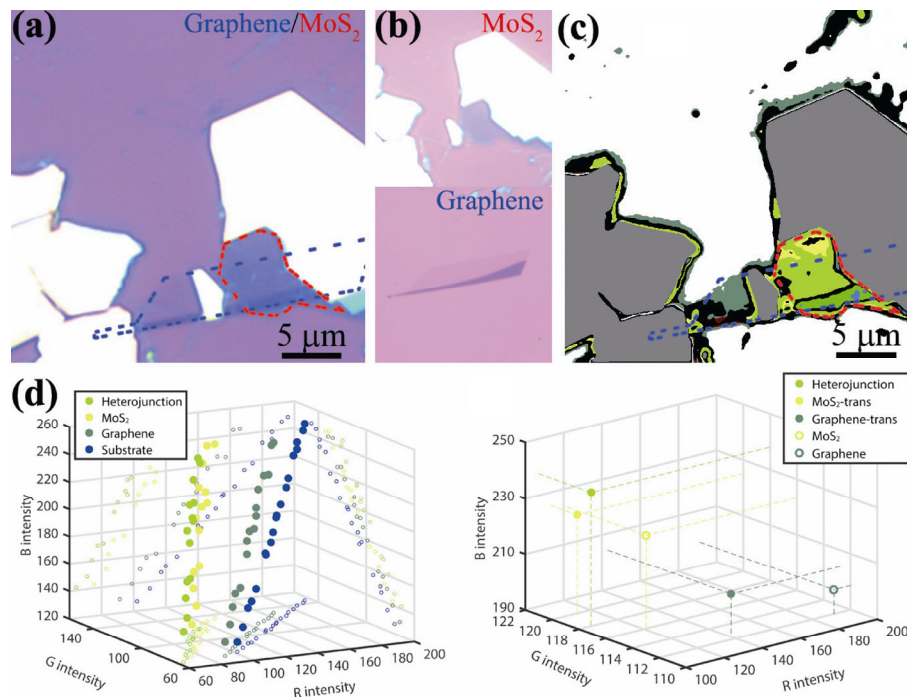


Figure 4 MOI of 2D heterostructure sample. (a) A 2D heterostructure with a vertical heterojunction of bilayer graphene and single-layered MoS₂, in which graphene and MoS₂ are marked respectively. (b) MoS₂ and graphene samples used to fabricate the heterostructure. (c) Test result of the heterostructure according to the training results of graphene and MoS₂, where graphene and MoS₂ are marked respectively. The as-identified regions of adhesive residues are blacked. (d) RGB information of heterojunction, graphene, and MoS₂ at different light intensities, where projections of 3D (RGB) data onto 2D plane (e.g., RG) are also plotted as circles. (e) Comparison of the RGB data of heterojunction, graphene, and MoS₂ at the same light intensity, together with the RGB data of graphene and MoS₂ before and after the transfer process.

materials and their heterostructures for additional physical properties (e.g., grain boundaries, defects, and interlayer coupling strength), as well as developments to meet the demands of autonomous fabrications. At the same time, artificial intelligence, especially machine-learning algorithm has been introduced for its great application potential in nanoscience and nanotechnology. The as-reported intelligent identification of 2D materials and heterostructures relies on the successful application of machine-learning strategy in optical microscopy analysis. With the ability of identifying subtle differences in the optical RGB information, this method can realize accurate and efficient identification of individual 2D materials with different thicknesses. The direct identification of RGB information collected from the optical photograph avoids possible influence of the color conversion process, which thus improves the identification accuracy in determining the existence of multiple 2D materials and even the impurities. By referring to the optical characteristics of 2D materials in RGB space, this method can simultaneously recognize different 2D materials and impurities, outperforming humans, in the characterization of 2D heterostructures, thereby boosting the corresponding device applications. Besides, such a machine-learning enhanced characterization method would promote the convergence of artificial intelligence and nanoscience by inspiring intelligent development of optical microscopy/spectroscopy and other characterization techniques.

4 Conclusions

In summary, we report the successful application of machine-learning strategy in the optical identification of 2D nanostructures, including graphene, MoS₂, and their heterostructures. The MOI method relies on trainable and automatic analyses of RGB information in the optical photograph of 2D nanostructures using a SVM algorithm. By endowing optical microscopy with intelligent insight into the characteristic color information of 2D materials and 2D heterostructures, the MOI method can realize accurate, intelligent, and large-area characterizations of 2D nanostructures, including the thickness, existence of resist residues, and even stacking order in heterostructures. With

applicability to wafer-scale 2D materials and 2D heterostructures, this intelligent identification method can certainly promote fundamental research and commercial level applications of 2D nanostructures.

5 Methods

5.1 Sample preparation and characterization

The graphene and the MoS₂ samples were fabricated by mechanical exfoliation on silicon wafers with 300 nm oxidation layers [40]. The heterostructure samples were prepared by a transfer and stacking method [35]. Characterizations of the samples were performed by AFM (Bruker, MultiMode 8), Raman spectroscopy (Horiba, Jobin-Yvon LabRAM HR800), and optical microscopy (Leica, DM2700 M). The self-customized software for the pretreatment, training, and testing processes was created using MATLAB.

5.2 Training process

All the 2D samples were photographed at different positions and light intensities to constitute the training set. Each photograph was then divided into sub-regions by the contour of the light intensity which was obtained from the photograph of the substrate (see Fig. S4 in the ESM) for the purpose of collecting more RGB information of the sample at different light intensities. Median and mean filters were first adopted in each picture for noise reduction followed by a color calibration treatment, i.e., scaling the G and B channel of all pixels in the whole photograph linearly based on a block of manually selected substrate as described above (see Fig. S5 in the ESM). Then, using a manually drawn mask for each photograph within the category for corresponding pixels (e.g., single layered graphene region), the mean value of each channel with the same category in one sub-region was calculated as the training dataset. Finally, a 3D one vs. one linear SVM can be trained to establish the model containing the characteristic RGB information (i.e., the “training result”) using the training dataset.

5.3 Test process

For the test process, denoising and color calibration treatments were also applied. The category of each

pixel can then be automatically identified referring to the training result based on their characteristic RGB information.

Acknowledgements

This work was supported by the National Natural Science Foundation of China (Nos. 51602013, 61602022 and 61627813), the National Basic Research Program of China (No. 2012CB932301), the International Collaboration 111 Project (No. B16001), Beijing Natural Science Foundation (No. 4162039) and funding support from Beijing Advanced Innovation Center for Big Data and Brain Computing (BDBC). The authors thank Ms. X. Y. Wang and Prof. Y. Lu for valuable discussions.

Electronic Supplementary Material: Supplementary material (SVM analyses of RGB information, optical characteristics of 2D materials in RGB space, theoretical calculation results of the optical contrast, contour of the light intensity in an optical microscopy photograph, color calibration treatment of the photograph and theoretical calculation of the optical contrast) is available in the online version of this article at <https://doi.org/10.1007/s12274-018-2155-0>.

References

- [1] Das Sarma, S.; Adam, S.; Hwang, E. H.; Rossi, E. Electronic transport in two-dimensional graphene. *Rev. Mod. Phys.* **2011**, *83*, 407–470.
- [2] Geim, A. K.; Novoselov, K. S. The rise of graphene. *Nat. Mater.* **2007**, *6*, 183–191.
- [3] Lin, X. Y.; Su, L.; Si, Z. Z.; Zhang, Y. G.; Bournel, A.; Zhang, Y.; Klein, J. O.; Fert, A.; Zhao, W. S. Gate-driven pure spin current in graphene. *Phys. Rev. Appl.* **2017**, *8*, 034006.
- [4] Novoselov, K. S.; Mishchenko, A.; Carvalho, A.; Castro Neto, A. H. 2D materials and van der Waals heterostructures. *Science* **2016**, *353*, aac9439.
- [5] Xia, F. N.; Wang, H.; Xiao, D.; Dubey, M.; Ramasubramanian, A. Two-dimensional material nanophotonics. *Nat. Photonics* **2014**, *8*, 899–907.
- [6] Geim, A. K.; Grigorieva, I. V. Van der Waals heterostructures. *Nature* **2013**, *499*, 419–425.
- [7] Zhang, Z. W.; Chen, P.; Duan, X. D.; Zang, K. T.; Luo, J.; Duan, X. F. Robust epitaxial growth of two-dimensional heterostructures, multiheterostructures, and superlattices. *Science* **2017**, *357*, 788–792.
- [8] Wu, T. R.; Zhang, X. F.; Yuan, Q. H.; Xue, J. C.; Lu, G. Y.; Liu, Z. H.; Wang, H. S.; Wang, H. M.; Ding, F.; Yu, Q. K. et al. Fast growth of inch-sized single-crystalline graphene from a controlled single nucleus on Cu-Ni alloys. *Nat. Mater.* **2015**, *15*, 43–47.
- [9] Xu, X. Z.; Zhang, Z. H.; Dong, J. C.; Yi, D.; Niu, J. J.; Wu, M. H.; Lin, L.; Yin, R. K.; Li, M. Q.; Zhou, J. Y. et al. Ultrafast epitaxial growth of metre-sized single-crystal graphene on industrial Cu foil. *Sci. Bull.* **2017**, *62*, 1074–1080.
- [10] Lee, J. H.; Lee, E. K.; Joo, W. J.; Jang, Y.; Kim, B. S.; Lim, J. Y.; Choi, S. H.; Ahn, S. J.; Ahn, J. R.; Park, M. H. et al. Wafer-scale growth of single-crystal monolayer graphene on reusable hydrogen-terminated germanium. *Science* **2014**, *344*, 286–289.
- [11] Huang, P. Y.; Ruiz-Vargas, C. S.; van der Zande, A. M.; Whitney, W. S.; Levendorf, M. P.; Kevek, J. W.; Garg, S.; Alden, J. S.; Hustedt, C. J.; Zhu, Y. et al. Grains and grain boundaries in single-layer graphene atomic patchwork quilts. *Nature* **2011**, *469*, 389–392.
- [12] Meyer, J. C.; Geim, A. K.; Katsnelson, M. I.; Novoselov, K. S.; Booth, T. J.; Roth, S. The structure of suspended graphene sheets. *Nature* **2007**, *446*, 60–63.
- [13] Zhao, W.; Xia, B. Y.; Lin, L.; Xiao, X. Y.; Liu, P.; Lin, X. Y.; Peng, H. L.; Zhu, Y. M.; Yu, R.; Lei, P. et al. Low-energy transmission electron diffraction and imaging of large-area graphene. *Sci. Adv.* **2017**, *3*, e1603231.
- [14] Zhang, Y. B.; Tang, T. T.; Girit, C.; Hao, Z.; Martin, M. C.; Zettl, A.; Crommie, M. F.; Shen, Y. R.; Wang, F. Direct observation of a widely tunable bandgap in bilayer graphene. *Nature* **2009**, *459*, 820–823.
- [15] Wastl, D. S.; Weymouth, A. J.; Giessibl, F. J. Atomically resolved graphitic surfaces in air by atomic force microscopy. *ACS Nano* **2014**, *8*, 5233–5239.
- [16] Tu, Q.; Lange, B.; Parlak, Z.; Lopes, J. M. J.; Blum, V.; Zauscher, S. Quantitative subsurface atomic structure fingerprint for 2D materials and heterostructures by first-principles-calibrated contact-resonance atomic force microscopy. *ACS Nano* **2016**, *10*, 6491–6500.
- [17] Ferrari, A. C.; Basko, D. M. Raman spectroscopy as a versatile tool for studying the properties of graphene. *Nat. Nanotechnol.* **2013**, *8*, 235–246.
- [18] Duong, D. L.; Han, G. H.; Lee, S. M.; Gunes, F.; Kim, E. S.; Kim, S. T.; Kim, H.; Ta, Q. H.; So, K. P.; Yoon, S. J. et al. Probing graphene grain boundaries with optical microscopy. *Nature* **2012**, *490*, 235–239.
- [19] Li, H.; Wu, J.; Huang, X.; Lu, G.; Yang, J.; Lu, X.; Xiong,

- Q. H.; Zhang, H. Rapid and reliable thickness identification of two-dimensional nanosheets using optical microscopy. *ACS Nano* **2013**, *7*, 10344–10353.
- [20] Li, W.; Moon, S.; Wojcik, M.; Xu, K. Direct optical visualization of graphene and its nanoscale defects on transparent substrates. *Nano Lett.* **2016**, *16*, 5027–5031.
- [21] Blake, P.; Hill, E. W.; Neto, A. H. C.; Novoselov, K. S.; Jiang, D.; Yang, R.; Booth, T. J.; Geim, A. K. Making graphene visible. *Appl. Phys. Lett.* **2007**, *91*, 063124.
- [22] Ni, Z. H.; Wang, H. M.; Kasim, J.; Fan, H. M.; Yu, T.; Wu, Y. H.; Feng, Y. P.; Shen, Z. X. Graphene thickness determination using reflection and contrast spectroscopy. *Nano Lett.* **2007**, *7*, 2758–2763.
- [23] Li, X. S.; Cai, W. W.; An, J. H.; Kim, S.; Nah, J.; Yang, D. X.; Piner, R.; Velamakanni, A.; Jung, I.; Tutuc, E. et al. Large-area synthesis of high-quality and uniform graphene films on copper foils. *Science* **2009**, *324*, 1312–1314.
- [24] Reina, A.; Jia, X. T.; Ho, J.; Nezich, D.; Son, H.; Bulovic, V.; Dresselhaus, M. S.; Kong, J. Large area, few-layer graphene films on arbitrary substrates by chemical vapor deposition. *Nano Lett.* **2009**, *9*, 30–35.
- [25] Lee, Y.; Lee, J.; Bark, H.; Oh, I.; Ryu, G. H.; Lee, Z.; Kim, H.; Cho, J. H.; Ahn, J.; Lee, C. Synthesis of wafer-scale uniform molybdenum disulfide films with control over the layer number using a gas phase sulfur precursor. *Nanoscale* **2014**, *6*, 2821–2826.
- [26] Zhao, M.; Ye, Y.; Han, Y. M.; Xia, Y.; Zhu, H. Y.; Wang, S. Q.; Wang, Y.; Muller, D. A.; Zhang, X. Large-scale chemical assembly of atomically thin transistors and circuits. *Nat. Nanotechnol.* **2016**, *11*, 954–959.
- [27] Alexeev, E. M.; Catanzaro, A.; Skrypka, O. V.; Nayak, P. K.; Ahn, S.; Pak, S.; Lee, J.; Sohn, J. I.; Novoselov, K. S.; Shin, H. S. et al. Imaging of interlayer coupling in van der Waals heterostructures using a bright-field optical microscope. *Nano Lett.* **2017**, *17*, 5342–5349.
- [28] Tan, Y.; Liu, X. B.; He, Z. L.; Liu, Y. R.; Zhao, M. W.; Zhang, H.; Chen, F. Tuning of interlayer coupling in large-area graphene/WSe₂ van der Waals heterostructure via ion irradiation: Optical evidences and photonic applications. *ACS Photonics* **2017**, *4*, 1531–1538.
- [29] Nolen, C. M.; Denina, G.; Teweldebrhan, D.; Bhanu, B.; Balandin, A. A. High-throughput large-area automated identification and quality control of graphene and few-layer graphene films. *ACS Nano* **2011**, *5*, 914–922.
- [30] Maxmen, A. Deep learning sharpens views of cells and genes. *Nature* **2018**, *553*, 9–10.
- [31] Christmann, A.; Steinwart, I. *Support Vector Machines*; Springer-Verlag: New York, 2008; pp 613.
- [32] Castellanos-Gomez, A.; Agrait, N.; Rubio-Bollinger, G. Optical identification of atomically thin dichalcogenide crystals. *Appl. Phys. Lett.* **2010**, *96*, 213116.
- [33] Zhu, F.; Lin, X. Y.; Liu, P.; Jiang, K. L.; Wei, Y.; Wu, Y.; Wang, J. P.; Fan, S. S. Heating graphene to incandescence and the measurement of its work function by thermionic emission method. *Nano Res.* **2014**, *7*, 553–560.
- [34] Castro Neto, A. H.; Guinea, F.; Peres, N. M. R.; Novoselov, K. S.; Geim, A. K. The electronic properties of graphene. *Rev. Mod. Phys.* **2009**, *81*, 109–162.
- [35] Lu, Z. X.; Sun, L. F.; Xu, G. C.; Zheng, J. Y.; Zhang, Q.; Wang, J. Y.; Jiao, L. Y. Universal transfer and stacking of chemical vapor deposition grown two-dimensional atomic layers with water-soluble polymer mediator. *ACS Nano* **2016**, *10*, 5237–5242.
- [36] Knittl, Z. *Optics of Thin Films: An Optical Multilayer Theory*; Wiley: London, 1976; pp 548.
- [37] Zhang, H.; Ma, Y. G.; Wan, Y.; Rong, X.; Xie, Z. A.; Wang, W.; Dai, L. Measuring the refractive index of highly crystalline monolayer MoS₂ with high confidence. *Sci. Rep.* **2015**, *5*, 8440.
- [38] Palik, E. D. *Handbook of Optical Constants of Solids*; Elsevier: Amsterdam, 1997.
- [39] Masubuchi, S.; Morimoto, M.; Morikawa, S.; Onodera, M.; Asakawa, Y.; Watanabe, K.; Taniguchi, T.; Machida, T. Autonomous robotic searching and assembly of two-dimensional crystals to build van der Waals superlattices. *Nat. Commun.* **2018**, *9*, 1413.
- [40] Novoselov, K. S.; Geim, A. K.; Morozov, S. V.; Jiang, D.; Zhang, Y.; Dubonos, S. V.; Grigorieva, I. V.; Firsov, A. A. Electric field effect in atomically thin carbon films. *Science* **2004**, *306*, 666–669.